Precise Modeling Based on Dynamic Phasors for Droop-Controlled Parallel-Connected Inverters

Wang, L.; Guo, X.Q. ; Gu, H.R.; Wu, W.Y.; Guerrero, Josep M.

Published in:
Proceedings of the 21st IEEE International Symposium on Industrial Electronics (ISIE), 2012

DOI (link to publication from Publisher):
10.1109/ISIE.2012.6237133

Publication date:
2012

Document Version
Early version, also known as pre-print

Precise Modeling Based on Dynamic Phasors for Droop-Controlled Parallel-Connected Inverters

L. Wang[1], X. Q. Guo[1], H.R. Gu[1], W.Y. Wu[1], and Josep M. Guerrero[2]
[1]Key Lab of Power Electronics for Energy Conservation and Motor Drive of Hebei Province, Yanshan University, PRC
E-mail: guoxq@ieee.org
[2]Institute of Energy Technology, Aalborg University, Denmark, E-mail: joz@et.aau.dk

***Abstract* – This paper deals with the precise modeling of droop controlled parallel inverters. This is very attractive since that is a common structure that can be found in a stand-alone droop-controlled MicroGrid. The conventional small-signal dynamic is not able to predict instabilities of the system, so that in this paper, the combination of both small signal model and dynamic phasor model (DPM) of parallel-connected inverters is presented. Simulation results show that the dynamic phasor model is able to predict accurately the stability margins of the system when the droop control gains exceed certain values. In addition, the virtual *ω-E* frame power control method, which deals with the power coupling caused by the line impedance X/R characteristic, has been chosen as an application example of this modeling technique.**

I. INTRODUCTION

Recently, distributed generation (DG) is drawing more and more attention. One step more is the MicroGrid concept, which encompasses distributed and storage generation units and loads in a local area. In an autonomous MicroGrid, all the DG units are responsible for maintaining the system voltage and frequency, while sharing the active and reactive power according to their own capacity. The proper control of an inverter is very important for this kind of applications. So that, a common approach for the parallel operation of inverters is the well known droop control.

The conventional droop control, which was derived from classical power system theory, is widely used in parallel inverters because it only needs to measure local signals, and no communication lines are needed. In the conventional droop control, the line impedance is considered to be mainly inductive. However, in low voltage grids the lines are mostly resistive, which may affect the way of controlling active and reactive power. Furthermore, the conventional droop control presents other drawbacks, so that many improved droop control methods are proposed in order to improve it.

The dynamic stability of inverter-based MicroGrid systems has been studied for many years. For that kind of applications, small-signal model is widely used since it is easy to predict the system response when changing parameters. Thus it is helpful to select control and system parameters. Furthermore, the MicroGrid configuration, operation modes, load position, and the inverters connection, affect the small signal-modeling and stability.

The modeling approach presented in [1] focuses on stability issues for an individual inverter connected to a stiff ac bus. Reference [2] creates the system level model, which includes all the variables in the entire MicroGrid, being the complexity very high. In [3], was assumed that the dynamics of the inner controllers can be neglected, thus making the model much more simple. This assumption is acceptable since the inner voltage and current controls bandwidth are much higher than the outer power loop used by the droop control, due to the low pass filter used by this loop. In [2] and [3], the results show that the droop gains play a significant role in the stability of the system. Another work [4] presents a small signal analysis for parallel connected inverters in stand-alone ac supply system with the conventional droop control, which makes stability and performance studies easier.

Summarizing, the model studied in [1]-[4], [8]-[9] neglects the dynamic of the power network circuit elements. This is acceptable for slow systems, such as multi-machine systems, but it can lead to questionable results for fast systems, such us inverters-based MicroGrid.

This paper presents a dynamic phasor model (DPM) for parallel connected inverters system. This model takes into account the dynamic of the power network circuit elements. The comparison between the small signal model by using the conventional modeling method and the DPM is performed by means of simulation results, showing the higher precision of the DPM.

Moreover, in order to deal with the active and reactive power coupling emphasized by the line impedance characteristic, the previously proposed virtual ω–E frame power control method is also studied here. For this case and the conventional one, the DPM is created, and the root locus analysis shows that this method can greatly improve the system stability. This paper is organized as follows. The system configuration and control scheme is shown in Section II. The small signal model is created in Section III. The DPM is proposed in Section IV. The sensitivity analysis and model is verified in Section V. Section VI presents the DPM of the virtual ω–E frame power control.

II. SYSTEM CONFIGURATION AND CONTROL SCHEME

The topology chosen for study is a MicroGrid operating in stand-alone mode. Fig.1 shows two inverters connected in parallel supplying all the power needed by the load while maintaining the voltage and frequency within the allowed range. In Fig. 1, E_n (n=1,2) and V are the amplitudes of the inverter output voltage and the ac bus voltage respectively, δ_n is the power angle difference, Z_n and θ_n are the magnitude and the phase of the line impedance respectively.

The overall control scheme contains inner voltage and current loops for regulating the inverter voltage, and external power loop for controlling the inverter output active and reactive power. The power loop uses the conventional droop control method.

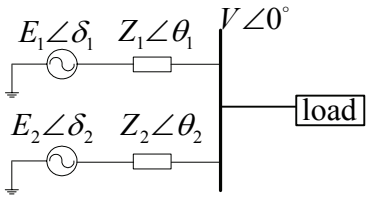

Fig. 1. A MicroGrid based on two inverters working in stand-alone mode

III. SMALL SIGNAL MODELING

In this section, a general procedure similar to that presented in [5] will be done in order to obtain the small signal model of the system described in Fig. 1. By using the conventional droop control, the inverter output frequency ω and the inverter output voltage E are controlled by means of the droop characteristics defined by:

$$\omega = \omega^* - k_p(P - P^*) \tag{1}$$

$$E = E^* - k_q(Q - Q^*) \tag{2}$$

being k_p and k_q the frequency and voltage droop coefficients, P and Q active and reactive power, and P^* and Q^* their respective references.

The inverter output active and reactive powers are given by [4], [5]:

$$P = \frac{3}{R^2 + X^2}(RE^2 - REV\cos\delta + XEV\sin\delta) \tag{3}$$

$$Q = \frac{3}{R^2 + X^2}(XE^2 - XEV\cos\delta - REV\sin\delta) \tag{4}$$

being R and X the resistive and inductive output impedance components, and δ the power angle.

For small disturbances around the equilibrium point (δ_e, E_e, V_e), the following linearized equations can be obtained:

$$\Delta\omega = \Delta\omega^* - k_p\Delta P + k_p\Delta P^* \tag{5}$$

$$\Delta E = \Delta E^* - k_q\Delta Q + k_q\Delta Q^* \tag{6}$$

$$\Delta P = k_{pe}\Delta E + k_{pd}\Delta\delta \tag{7}$$

$$\Delta Q = k_{qe}\Delta E + k_{qd}\Delta\delta \tag{8}$$

where

$$k_{pe} = \frac{3RE}{R^2 + X^2} \tag{9}$$

$$k_{pd} = \frac{3XE^2}{R^2 + X^2} \tag{10}$$

$$k_{qe} = \frac{3XE}{R^2 + X^2} \tag{11}$$

$$k_{qd} = \frac{-3RE^2}{R^2 + X^2} \tag{12}$$

To measure the inverter output active and reactive power, a low pass filter is often used. Thus, the active and reactive powers obtained by averaging over a line frequency using a low pass filter can be represented by (13) and (14):

$$\Delta p = \frac{\omega_f}{s + \omega_f}\Delta P \tag{13}$$

$$\Delta q = \frac{\omega_f}{s + \omega_f}\Delta Q \tag{14}$$

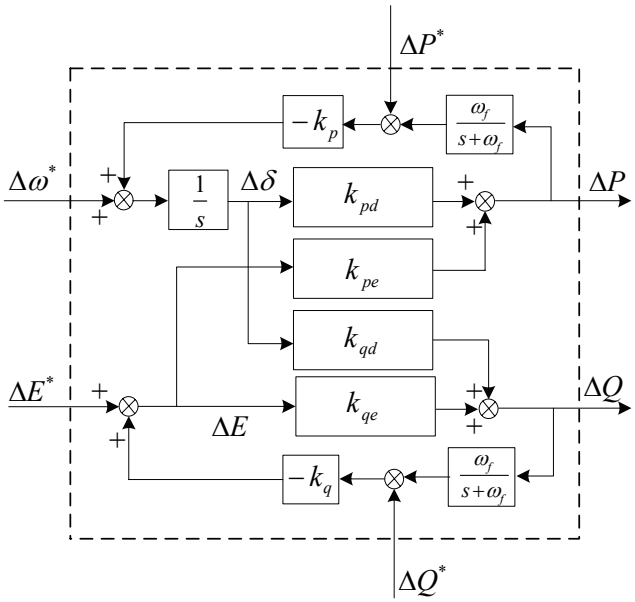

Fig. 2. Small signal close-loop model

From (1)-(8) it is possible to sketch the small signal closed-loop model as shown in Fig. 2. The references ω^*, E^*, P^*, and Q^* are considered to be constant here, so their deviation term in (5) and (6) can be neglected.

Due to the low pass filter, the inner voltage and current control bandwidth are much higher than the outer power loop. So that, it can be assumed that the dynamic of the inner loops can be neglected. Thus, the inverter output voltage is considered to be directly governed by the references generated by the droop control strategy.

Considering above the assumption, by combining (5)-(14), we can get the following equations.

$$\Delta\omega = -\frac{k_p\omega_f}{s + \omega_f}(k_{pe}\Delta E + k_{pd}\Delta\delta) \tag{15}$$

$$\Delta E = -\frac{k_q\omega_f}{s + \omega_f}(k_{qe}\Delta E + k_{qd}\Delta\delta) \tag{16}$$

The phase angle is the integration of the frequency, as shown in (17).

$$\Delta\omega = s\Delta\delta \tag{17}$$

By combining of (15)-(17), the characteristic equation of the close loop system with the conventional droop is obtained as in (18).

$$s^3 + as^2 + bs + c = 0 \tag{18}$$

where

$$a = (2 + k_q k_{qe})\omega_f \tag{19}$$

$$b = (k_p k_{pd} + k_q k_{qe}\omega_f + \omega_f)\omega_f \tag{20}$$

$$c = (k_{pd} + k_q k_{pd} k_{qe} - k_q k_{pe} k_{qd}) k_p \omega_f^2 \quad (21)$$

The coefficient in (18) determines the roots and therefore the closed loop stability.

IV. DYNAMIC PHASOR MODELING

The small signal model described in Section III neglects the dynamic of the power network circuit elements. This model is acceptable for high inertial systems, but it can lead to questionable results for power electronics inverter based system. To deal with this problem, this Section proposes the dynamic phasors based model.

The concept of dynamic phasors has been developed for a balanced, three-phase power system, enabling the inclusion of the network dynamics as in [6]. In this section, this technique is used to create the small signal model of the system shown in Fig.1. This modeling will be called hereinafter DPM.

The dynamic or time-varying phasor (X_k) can be expressed in its integral form defined inside the interval $\tau \in (t-T, t]$ by means of [10]:

$$X_k(t) = \frac{1}{T}\int_{t-T}^{t} x(\tau) e^{-jk\omega_s \tau} d\tau = \langle x \rangle_k (t) \quad (22)$$

Then derivative with respect to time of the k^{th} dynamic phasor X_k can be expressed as following:

$$dX_k(t)/dt = \langle dx/dt \rangle_k (t) - jk\omega_s X_k(t) \quad (23)$$

Then the relationship between inductor voltage v_L and the current through the inductor i_L can be expressed by:

$$v_L = L(di_L/dt) + j\omega L i_L \quad (24)$$

In the conventional circuit theory, the second term on the right hand of (24) does not existent.

Based on (24), the inverter output active and reactive power can be expressed by:

$$P = 3\frac{Ls+R}{(Ls+R)^2+(\omega L)^2}(E^2 - EV\cos\delta) + 3\frac{\omega L}{(Ls+R)^2+(\omega L)^2} EV\sin\delta \quad (25)$$

$$Q = 3\frac{\omega L}{(Ls+R)^2+(\omega L)^2}(E^2 - EV\cos\delta) - 3\frac{Ls+R}{(Ls+R)^2+(\omega L)^2} EV\sin\delta \quad (26)$$

For small disturbances around the equilibrium point (δ_e, E_e, V_e), the linearized equations in (27) and (28) can be obtained.

$$\Delta P = k'_{pe}\Delta E + k'_{pd}\Delta\delta \quad (27)$$

$$\Delta Q = k'_{qe}\Delta E + k'_{qd}\Delta\delta \quad (28)$$

where

$$k'_{pe} = \frac{3(Ls+R)E}{(Ls+R)^2+(\omega L)^2} \quad (29)$$

$$k'_{pd} = \frac{3\omega L E^2}{(Ls+R)^2+(\omega L)^2} \quad (30)$$

$$k'_{qe} = \frac{3\omega L E}{(Ls+R)^2+(\omega L)^2} \quad (31)$$

$$k'_{qd} = \frac{-3(Ls+R)E^2}{(Ls+R)^2+(\omega L)^2} \quad (32)$$

Through (5), (6), (13), (14), (17), (27), and (28), the DPM characteristic equation can be obtained as in (33).

$$a's^5 + b's^4 + c's^3 + d's^2 + e's + f' = 0 \quad (33)$$

where

$$a' = L^2 \quad (34)$$

$$b' = 2RL + 2\omega_f L^2 \quad (35)$$

$$c' = R^2 + \omega^2 L^2 + 4RL\omega_f + L^2\omega_f^2 \quad (36)$$

$$d' = 2R^2\omega_f + 2\omega_f\omega^2 L^2 + 2RL\omega_f^2 + 3\omega LEk_q\omega_f \quad (37)$$

$$e' = R^2\omega_f^2 + \omega^2 L^2\omega_f^2 + 3\omega LEk_q\omega_f^2 + 3\omega LE^2 k_p\omega_f \quad (38)$$

$$f' = 3\omega LE^2 k_p\omega_f^2 + 9E^3 k_p k_q \omega_f^2 \quad (39)$$

The coefficient in (33) determines the roots and therefore the closed loop stability.

V. SENSITIVITY ANALYSIS AND MODEL VERIFICATION

Section III presents the small signal model using the conventional way, while Section IV proposes the DPM using dynamic phasors technique. In this Section, a sensitivity analysis is conducted by using both models. The small signal model is a three-order system, while the DPM is a five-order system. Simulation will be conducted by using the system shown in Fig. 1, in order to show which model is more accurate.

The system parameters used in this analysis are shown in Table I. For the analysis, it has been considered that the capacity of inverter #1 is two times bigger than the capacity of inverter #2. The active power droop gain of inverter #1, k_p, has been changed from 0.0001 to 0.5, and the reactive power droop gain of inverter #1 k_q is also changed from 0.0001 to 0.5. The droop gains of inverter #2 are two times more than that of inverter #1, accordingly.

Fig. 3 shows the root locus comparison of the two models as k_p increasing. The small signal model shows that all the poles are in the left half plane, while the DPM shows that some of the poles move to right half plane, which will cause the system unstable. Simulation results by using the parameters of the green circle (k_p=0.01) and the red circle (k_p=0.05) in Fig. 3, are shown in Fig. 4. It can be seen that the system is stable when k_p is 0.01, while unstable when k_p is 0.05. The simulation results are consistent with the DPM.

Fig. 5 shows the root locus comparison of the two models when increasing k_q. The small signal model shows that all the poles are in the left half plane, while the DPM shows that some of the poles move toward the right half plane and may cause the system unstable. Simulation results using the parameters of the green circle (k_q=0.1) and the red circle (k_q=0.5) in Fig. 5, are shown in Fig. 6. It can be seen that the system is stable when k_q is 0.1, while unstable when k_q is 0.5. Here also the simulation results are consistent with the DPM.

Through the simulation results, we can draw the conclusion that the dynamic model is more precise than the small signal model, which is not able to predict that stability limit.

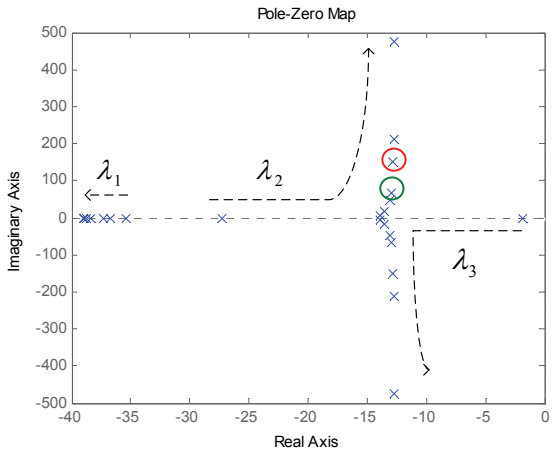

(a) small signal model

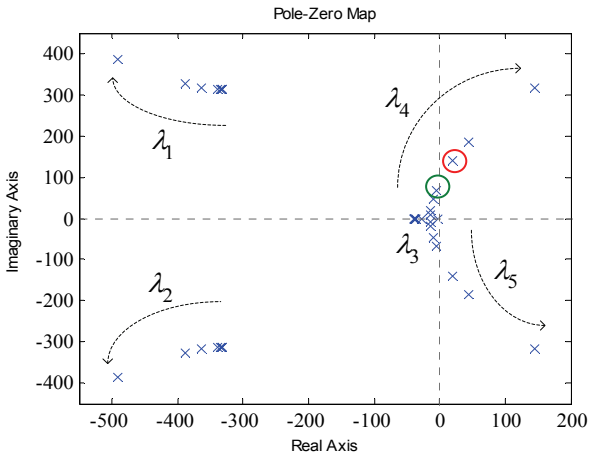

(b) DPM

Fig. 3. Root locus comparison for k_p variations.

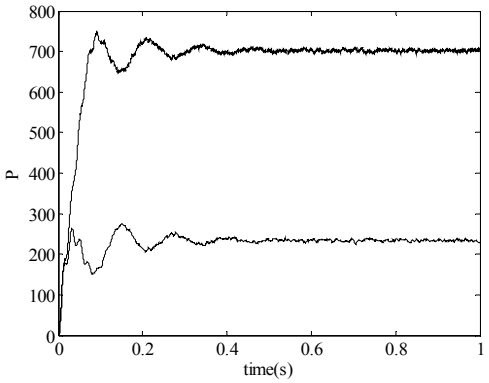

(a) $k_p = 0.01$

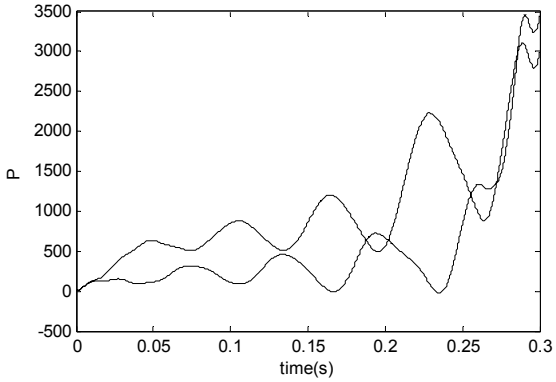

(b) $k_p = 0.05$

Fig, 4. The inverters output active power for k_p variations.

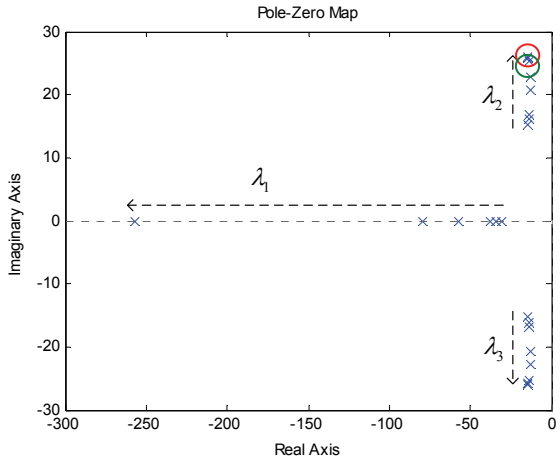

(a) small signal model

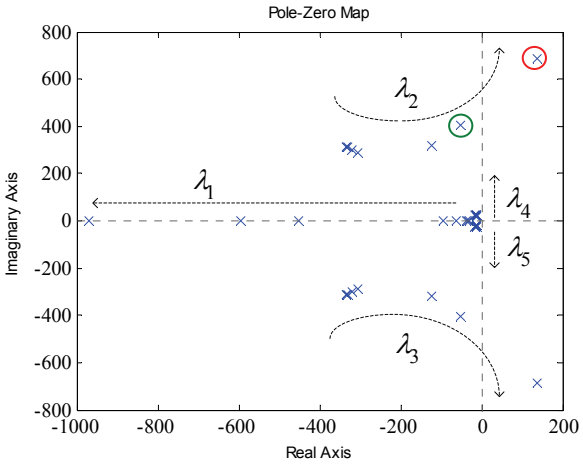

(b) DPM

Fig. 5. Root locus comparison for k_q variations.

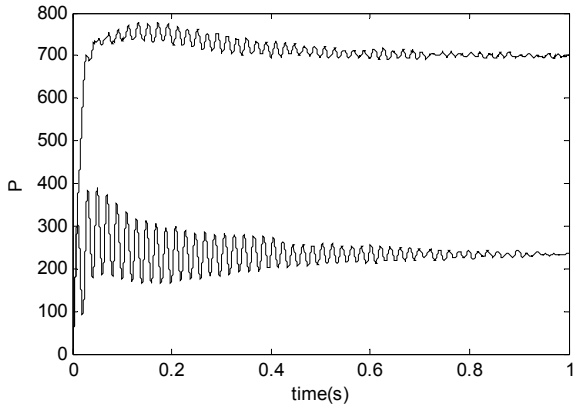

(a) $k_q = 0.1$

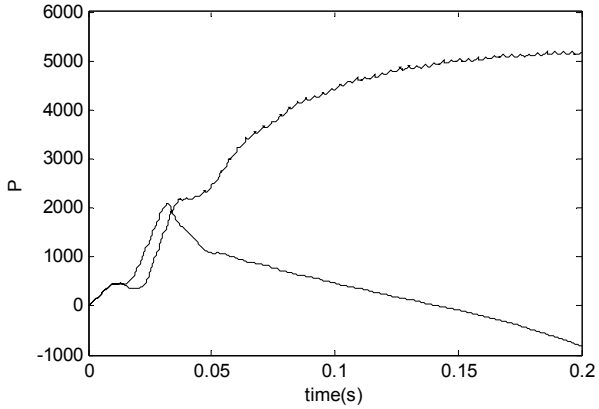

(b) $k_q = 0.5$

Fig. 6. The inverters output active power for k_q variations.

TABLE I. SYSTEM PARAMETERS

Parameter	Value
DC link voltage	250V
filter inductance	3mH
filter conductance	9.9μF
line impedance	1+j 1Ù
output voltage	100V
output frequency	50Hz
low pass filter frequency	30rad/s

VI. DYNAMIC PHASOR MODEL OF POWER DECOUPLING DROOP METHOD

In this Section, an illustrative example of application of the DPM approach is presented. From Fig. 2 it can be seen that by using the conventional droop control, when adjusting the voltage amplitude or frequency will affect both active and reactive power, thus no decoupling can be achieved. The conventional droop control assumed that the line impedance is mainly inductive, but when the line resistive can no longer be neglected, so that the conventional droop control will emphasize more the power coupling.

Many improved droop control methods have been proposed in order to deal with the power coupling problem in the recent years. A method called virtual ω–E frame power control, proposed in [7], is very effective. In this Section, DPM is used to study the stability of this droop control method.

By using the virtual ω–E frame power control, the inverter output frequency ω and the inverter output voltage E are controlled by the following droop characteristics:

$$\omega' = \omega'^{*} - k_p(P - P^{*}) \tag{40}$$

$$E' = E'^{*} - k_q(Q - Q^{*}) \tag{41}$$

where

$$\begin{bmatrix} \omega' \\ E' \end{bmatrix} = \begin{bmatrix} \cos\varphi & \sin\varphi \\ -\sin\varphi & \cos\varphi \end{bmatrix} \begin{bmatrix} \omega \\ E \end{bmatrix}, \varphi = 90^{\circ} - \theta$$

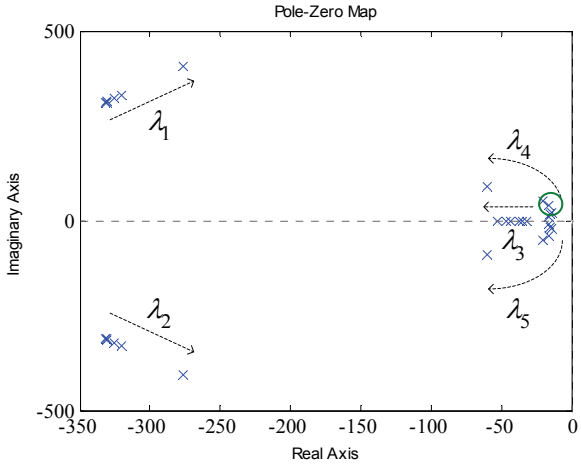

Fig. 7. Root locus family of the DPM with virtual ω-E frame power control for k_p variations.

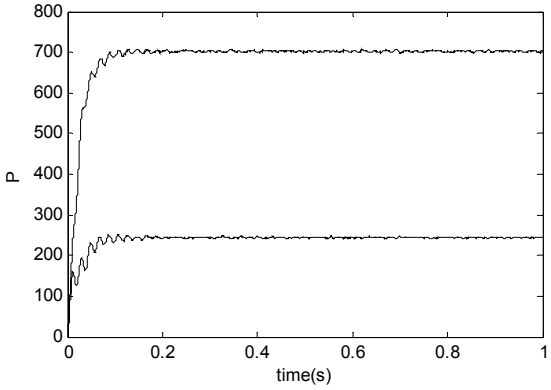

Fig, 8. The inverters output active power with the virtual ω–E frame power control when k_p is 0.05

For small disturbances around the equilibrium point (δ_e, E_e, V_e), the linearized equations following can be obtained:

$$\Delta\omega\cos\varphi + \Delta E\sin\varphi = -k_p\Delta P \tag{42}$$

$$\Delta E\cos\varphi - \Delta\omega\sin\varphi = -k_q\Delta Q \tag{43}$$

Through (13), (14), (17), (27), (28), (42), and (43), the DPM characteristic equation can be obtained as:

$$a''s^5 + b''s^4 + c''s^3 + d''s^2 + e''s + f'' = 0 \tag{44}$$

where

$$a^{"} = L^2 \tag{45}$$

$$b^{"} = 2RL + 2\omega_f L^2 \tag{46}$$

$$c^{"} = R^2 + \omega^2 L^2 + 4RL\omega_f + L^2\omega_f^2 + 3k_p\omega_f LE\sin\varphi \tag{47}$$

$$d^{"} = 2R^2\omega_f + 2\omega_f\omega^2 L^2 + 2RL\omega_f^2 + 3k_q\omega_f E^2 L\sin\varphi + 3k_q\omega_f\omega LE\cos\varphi + 3k_p\omega_f^2 LE\sin\varphi + 3k_p\omega_f RE\sin\varphi \tag{48}$$

$$e^{"} = R^2\omega_f^2 + \omega^2 L^2\omega_f^2 + 3k_q\omega_f^2 E^2 L\sin\varphi + 3k_q\omega_f E^2 R\sin\varphi + 3k_q\omega_f^2\omega LE\cos\varphi + 3k_p\omega_f^2 RE\sin\varphi + 3k_p\omega_f\omega LE^2\cos\varphi \tag{49}$$

$$f^{"} = 3k_q\omega_f^2 E^2 R\sin\varphi + 3k_p\omega_f^2\omega LE^2\cos\varphi + 9k_p k_q\omega_f^2 E^3 \tag{50}$$

It is our worth to note that when the line impedance angle is 90 degrees, then φ is 0 degrees, and in this situation the characteristic equation in (44) is exactly the same as the one shown in (33).

Fig. 7 shows the root locus of the DPM of the closed loop system when using the virtual ω–E frame power control for k_p variations. By comparing Fig. 7 with Fig. 3(b), it can be seen that the dynamic response is much faster than the conventional droop control. Notice that for this control approach all the poles are at the left half plane, so that the system is stable. Simulation result when using the virtual ω–E frame power control is shown in Fig. 8, k_p is 0.05 here. It can be observed that by using the power decoupling droop method, the system stability is greatly improved.

VII. CONCLUSION

In this paper, the stability of the stand-alone droop-controlled MicroGrid is discussed. Based on a two parallel inverter system, the small signal model and the DPM are obtained and compared. The small signal model shows that the system keeps stable even when using large droop gains, however, the large signal simulation results show that this is not true. Thus, small signal model is not precise enough to study the dynamics and stability of the closed loop system.

To deal with the model precise problem, a dynamic phasors based approach is used. This method takes the dynamic of the power network circuit elements into account. Simulation results show that this model can be used to accurately predict the system stability limits. Hence, we can obtain the droop gains that make the system stable, while the small signal model failed to do so. As a result, we can conclude that DPM is more precise and can be used to design the parameters of the real system.

Finally, the proposed modeling approach can be used for other control techniques. As an example, in order to deal with the power coupling caused by the line impedance, virtual ω–E frame power control method is analyzed. Thus, DPM was obtained, and the root locus shown that this method can greatly improve the system stability.

ACKNOWLEDGMENT

This work was supported by the National Natural Science Foundation of China (50837003, 50977081), Hebei Province Universities Science Research Project (2011249) and Hebei Province Natural Science Foundation (E2012203023).

REFERENCES

[1] J.M.Guerrero, L.G.V.na,M.Catilla, and J.Miret, "A wireless controller to enhance dynamic performance of parallel inverters in distributed generation systems," *IEEE Transactions on Power Electronics,* vol. 19, no.5, pp. 1205-1213, Sept. 2004.

[2] N.Pogaku, M,Prodanovic, and T.Green, "Inverter-based microgrids: Small-signal modeling and testing," *Power Electronics, Machines and Drives,2006. The 3rd IET International Conference*, pp. 499-504, Mar. 2006.

[3] Shivkumar V.Iyer, Madhu N.Belur, and Mukul C.Chandorkar, "A generalized computational method to determine stability of a multi-inverter microgrid," *IEEE Transactions on Power Electronics,* vol. 25, no.9, pp. 2420-2432, Sept. 2010.

[4] E.Coelho, P.Cortizo, and P.Garcia, "Small-signal stability for parallel-connected inverters in stand-alone ac supply systems," *IEEE Transactions on Industry Applications,* vol. 38, no.2, pp. 533-542, March/April. 2002.

[5] E.Coelho, P.Cortizo, and P.Garcia, "Small signal stability for single phase inverter connected to stiff ac system," *Proc.IEEE IAS. Annual.Meeting.* 1999. pp. 2180-2187.

[6] K.De Brabandere, B.Bolsens, J.Van den Keybus, J.Driesen, M.Prodanovic, and R. Belmans, "Small-signal stability of grids with distributed low-inertia generators taking into account line phasor dynamics," in IET 18th *International Conference and Exhibition on Electricity Distribution,* CIRED 2005, pp. 1-5.

[7] Y.Li, Y.W.Li, "Decoupled power control for an inverter based low voltage microgrid in autononmous operation," *Power Electronics and Motion Control Conferenc,2009. IPEMC'09. IEEE 6th International* ,2009. pp. 2490-2496.

[8] Filho, R.M.S.; Seixas, P.F.; Cortizo, P.C.; Gateau, G., "Small-signal stability enhancement of communicationless parallel connected inverters," Industrial Electronics, 2009. IECON '09. 35th Annual Conference of IEEE , vol., no., pp.863-870, 3-5 Nov. 2009

[9] Vasquez, J.C.; Guerrero, J.M.; Luna, A.; Rodriguez, P.; Teodorescu, R., "Adaptive Droop Control Applied to Voltage-Source Inverters Operating in Grid-Connected and Islanded Modes," Industrial Electronics, IEEE Transactions on , vol.56, no.10, pp.4088-4096, Oct. 2009.

[10] Dragan Maksimovic, Aleksandar M. Stankovic, V. Joseph Thottuvelil, and George C. Verghese, "Modeling and Simulation of Power Electronic Converters," *PROCEEDINGS OF THE IEEE,* vol. 89, no.6, pp. 898-912, Jun. 2001.